Stackelberg Game-Based Deployment Design and Radio Resource Allocation in Coordinated UAVs-Assisted Vehicular Communication Networks

Maryam Hosseini and Reza Ghazizadeh

***Abstract*—This paper studies optimum deployment design and radio resource allocation in a coordinated unmanned aerial vehicle (UAVs)-assisted vehicular communication network. The scarcity of radio resources and the lack of appropriate communication paths have been challenging in the existing vehicular networks. Although employing UAVs with well-designed deployments can support vehicular communications by providing line-of-sight (LoS) links, however, limited energy and spectrum scarcity issues motivate us to apply non-orthogonal multiple access (NOMA) with successive-interference-cancellation (SIC) as a solution to enhance radio resource efficiency for downlink infrastructure-to-vehicle (I2V) links. Meanwhile, due to the high complexity of the overall optimization problem that jointly handles deployment design and resource allocation for the studied UAVs-assisted vehicular network, we propose a low-complexity hierarchical suboptimal solution method. First, to efficiently find the optimum deployment of UAVs, we propose Stackelberg game with competitive nature as a game theory-based method, where UAVs are divided into leaders and followers groups that compete with each other to obtain the optimal position. Subsequently, we perform a low-complexity dynamic method in which radio resources are allocated in a sub-channel assignment algorithm and in a power allocation problem, respectively. Finally, the closed-form expressions of the optimal power allocation are derived using the KKT optimality conditions. Simulation results demonstrate improved performance for deployment design using the Stackelberg game. It is shown that NOMA improves the achievable sum rate compared to conventional orthogonal multiple access (OMA). Also, fast convergence of the proposed resource allocation and deployment design is obtained.**

***Index Terms*—Vehicular communication network, UAV, Stackelberg game, NOMA, radio resource allocation.**

I. Introduction

DUE to the fast-growing demands of mobile data traffic on roads, vehicular communication networks with foundations of infrastructure-to-vehicle (I2V) and vehicle-to-vehicle (V2V) communication links have attracted significant interest in wireless research communities [1], [2], [3], [4], [5], [6]. The main advantages of vehicular communications are improving safety and connectivity, and providing entertainment (such as online games and video streaming) for passengers on the road. To address these goals, a high-reliability connection of vehicles with cellular infrastructure must be provided. To improve the connection quality between vehicles in vehicular networks, [7] suggested that some vehicles act as mobile base stations (BSs). Thereby, vehicles such as trucks and buses were considered as mobile-femtocell access points (FAPs) to support vehicles within their coverage area. Although this work well demonstrated the efficiency of the proposed connectivity solution in the case with mobile FAPs, the path availability in many other cases is still an unknown issue. Also, due to the high mobility nature of vehicular networks, the availability of cellular infrastructures for such networks is a challenging problem [8]. Employing unmanned aerial vehicles (UAV) as aerial BS or relay is envisioned as a promising solution to overcome these challenges.

The UAV, commonly known as a drone, due to its potential for high mobility, flight altitude adjustment, on-demand deployment, and cost-effectiveness, has attracted the focus of wireless researchers as an enabling technology to facilitate communications for some terrestrial wireless networks [9], [10], [11]. Authors in [12] studied a UAV-enabled multicast channel, in which a UAV as an aerial transmitter serves a group of ground users. They characterized the capacity of the channel link as subject to the power and speed constraints over a finite period. To support the massive connectivity of moving vehicles, the UAV especially thanks to free mobility and flexible deployment can be considered as promising assistance for vehicular communication networks and can offer a robust I2V link to enhance channel quality [13], [14], [15], [16]. In addition, by providing a good line of sight (LoS) link [4], [17], the UAV as an aerial cellular infrastructure can support vehicular communication, especially in scenarios with hazardous environments, massive temporary traffic, and other cases where the ground cellular infrastructure is temporarily unavailable [9], [18], [19]. Besides, employing the UAV can overcome the route dependence on vehicle density and cooperation among vehicles [20]. The authors in [20] demonstrated that the UAV enhances the availability of the connection path and thus decreases the data-packet delivery delay. It was also shown that the scheme without UAV is highly dependent on the density of vehicles, while in the scheme with the UAV, increasing in the number of vehicles does not have a significant impact on the connectivity-path availability.

Besides all advantages of a single UAV as an aerial base station, it faces many challenges to be addressed. One important issue is that most capabilities of a UAV are subject to its limited

Manuscript received 23 April 2022; revised 1 August 2022; accepted 1 September 2022. Date of publication 12 September 2022; date of current version 16 January 2023. The review of this article was coordinated by Dr. Wei Quan. *(Reza Ghazizadeh is co-first author.) (Corresponding author: Maryam Hosseini.)*

The authors are with the Department of Electrical and Computer Engineering, University of Birjand, Birjand 9717434765, Iran (e-mail: maryam.hosseini@birjand.ac.ir; rghazizade@birjand.ac.ir).

Digital Object Identifier 10.1109/TVT.2022.3206145

energy and coverage area. Therefore, a single UAV cannot support a huge and high-mobility wireless communications system such as a vehicular network [9]. To tackle this issue, we are motivated to use multiple UAVs that dynamically are coordinated as a network with enhanced capabilities compared to a single UAV, and as a result, the efficiency of the served systems is improved [11], [21], [22], [23]. In order to enhance the capabilities of multi-UAV networks, the trajectory design, coverage issues, and resource allocation become fundamental problems in an efficient deployment. The authors in [13], studied the optimization of trajectory and resources for UAVs that support a communication network where cellular services are not available. They considered a downlink scenario in which the UAVs communicate with multiple users simultaneously, by employing orthogonal frequency-division multiple access (OFDMA). Also, in [24] a multi-UAV-assisted wireless communication system was considered. With the aim of fairness among users, the authors maximized the minimum throughput among all users by optimizing user scheduling, and jointly optimizing UAVs trajectories and power allocation. They solved the problem with an efficient iterative algorithm with convergence guarantee and achieved throughput gains. Numerical results in this paper showed that flying UAVs enhance the throughput of the communication system compared to the conventional case with static ground BS. However, the study in [24] focused on the static network users and thus did not take advantage of the capabilities of UAVs such as agility and free mobility to efficiently support a high-mobility network. Moreover, it was assumed that in each time slot, each UAV serves at most one user, and hence the aspect of resource efficiency was not well addressed.

Meanwhile, with the enhancement of wireless network capabilities and the fast-growing demands of mobile data traffic, a promising resource access technique is needed to improve the efficiency of available radio resources. The conventional orthogonal multiple access (OMA) method, where every resource block is exclusively allocated to a single user, cannot meet all the radio resource needs [25], [26]. To overcome the radio resource scarcity issues, we consider the non-orthogonal multiple access (NOMA) technique that in contrast to OMA, allows multiple users to share the same spectrum resource block simultaneously and leads to enhanced spectral and energy efficiency [27], [28], [29], [30], [31], [32], [33], [34]. By performing successive interference cancellation (SIC) in a NOMA system where the receivers observe strong interference, the desired signal can be correctly detected from superposition coded signal at the destination [32], [35], [36]. In [34], the problem of joint user assignment and uplink power allocation exploiting the NOMA technique was studied. The user-BS association was obtained in an iterative and distributed method. Then, the optimal power allocation was obtained in order to optimize the BSs' utility functions while satisfying the optimality of the associated users' utility functions. By applying NOMA to vehicular networks, multiple I2V links are multiplexed into the power domain (considering the channel gain differences) and then, non-orthogonally are scheduled for transmission on the same spectrum resource block [15], [32]. Hence, using NOMA leads to the efficient assignment of the radio resources and as a result, massive connectivity in vehicular communication networks can be provided [37], [38]. In [39], NOMA was performed along with SIC in a vehicular communication network. Then, small cell BS assignment and power allocation were investigated to maximize system utility aiming to enhance the long-term performance of the system and to decrease the hand-over rate. Improved spectrum-energy efficiency was achieved for the joint optimization of user assignment and power allocation. Despite the significant effort spent on applying NOMA to vehicular networks in [39], important vehicular network issues such as communication path availability were not considered. Although employing UAVs as aerial infrastructure can overcome this issue, the dynamic nature of UAVs along with the complexity of the NOMA technique causes further computational challenges in such systems that should be well addressed.

To deal with the high complexity of optimization problems in these challenging networks, finding and using a creative solution method has always been one of the main challenges for researchers. In [14], considering the UAV as a temporary BS, a Q-Learning algorithm was performed to control the trajectory of the UAV in order to optimally adapt the time-varying channel. In part of [40], a deep reinforcement learning-based computing offloading policy is proposed to deal with system complexity in a dynamic space-air-ground integrated network (SAGIN), where UAVs enable near-user edge computing and satellites support access to cloud computing. Authors in [41] investigated and formulated the resource allocation problem in a multi-cell multicarrier NOMA network. To solve the challenging formulated problem, they proposed a three-dimensional (3D) matching algorithm to model the relation among users, BSs, and sub-channels, and then effectively solved the problem. Game theory-based methods are also effective tools for solving complex problems in a wide range of science fields [42], [43], [44]. In [42], the authors presented a centralized-distributed game-theoretic framework for an energy-efficient coverage deployment design in a multi-cooperative UAV system. They decomposed the proposed scheme into the phases of coverage maximization and power control, both of which can be solved sub-optimally by low-complexity games. The work in [44] proposed a game-theoretic approach to improve energy efficiency in a distributed NOMA-based public safety network. The Stackelberg game by breaking the challenging problems into several sub-problems with low complexity can tackle the high computation and high-complexity. In [43], Stackelberg game-based optimization problems were formulated to maximize the achievable sum rate of a NOMA system. The authors analyzed the complexity and convergence of the proposed algorithms. As shown in [43], promising performance was obtained using the Stackelberg game-based method.

A. Motivation and Contributions

The high mobility nature of vehicular networks motivates the employment of flying UAVs to overcome communication path unavailability issues via the LoS links. Furthermore, the conventional OMA system cannot efficiently meet all wireless demands in such ongoing vehicular networks. There are some works that study jointly deployment design and resource allocation in UAV-enabled static wireless networks such as [24], [45], or investigate deployment design and user association problem in NOMA-based UAV-assisted static network [22].

Also, there are a few research contributions that study applying the NOMA technique in a single UAV-assisted vehicular network such as [15]. However, the dynamic deployment design of several cooperative UAVs, with joint user assignment and resource allocation based on the NOMA system for vehicular communications has not been well investigated due to the high computational complexity, especially for such high mobility networks. This work proposes a hierarchical suboptimal scheme including a game-theoretic method that facilitates deployment design, user assignment, and resource allocation based on NOMA in the coordinated UAVs-assisted vehicular networks. The main contributions of this paper are listed as follows:

- We design a multi-cell NOMA-UAV network deployment, where UAVs are coordinated to serve vehicular communications in a situation in which the static ground infrastructures are unavailable while the efficient radio resources allocation is performed. Our approach considers that all UAVs share the same frequency band and only focuses on the downlink transmission, slowly varying and large-scale fading CSI of I2V links.
- Due to applying NOMA, a received signal on each resource block is subject to both intra-cell interferences caused by co-channel and co-cell I2V links, and inter-cell interferences caused by co-channel I2V links from the adjacent cells. The cancellation of both inter-cell and intra-cell co-channel interferences motivates us to perform the SIC technique at the receivers to successively cancel interferences based on the difference in transmission power domain.
- We aim to maximize the average data transmission rate by jointly optimizing the user assignment, UAVs deployment design, and radio resources allocation, which leads to a mixed-integer nonlinear programming (MINLP) problem.
- To solve the challenging optimization problem, we propose a hierarchical suboptimal scheme that includes a game theory-based method. First, UAV-vehicle assignment is facilitated via a low-complexity algorithm. Next, the optimum deployment of UAVs is found by performing the Stackelberg game method. In this game, UAVs exploiting potentials such as free mobility and flexible deployment compete with each other as the game players to find their optimal position. Then, exploiting the channel gain differences among I2V links, all vehicles in each cell are grouped into multiple clusters, and each cluster is matched to the most appropriate resource block based on the minimization of co-channel interference. Finally, the power allocation problem is formulated for each cluster, and closed-form expressions for power allocation for different cluster sizes are derived using the KKT optimality conditions.
- We study the convergence and computational complexity of the proposed algorithms. We expect that the proposed algorithms converge quickly for a system setup with a moderate number of users. Also, it is demonstrated that the computational complexity for the proposed scheme is very low compared to the exhaustive search method.
- Simulation results evaluate the presented scheme and compare its performance with other benchmark schemes such as OMA and static UAVs. The superior performance of the NOMA method compared to the conventional OMA scheme is demonstrated. Besides, the effectiveness of the proposed algorithm along with the Stackelberg game is shown in terms of the sum-achievable rate compared to the case of static UAVs. Also, the fast convergence of the proposed algorithms for the studied scenario is shown.

TABLE I
A SUMMARY OF MAIN NOTATIONS

Notation	Description
J	Number of vehicles
I	Number of UAVs
K	Number of resource blocks
J_K	Number of co-channel users (NOMA factor)
N_i	Total number of vehicles connected to UAV$_i$
T	Time duration (sec)
Δt	The size of each time slot (ms)
N_t	Number of time slots
B_T	Total available bandwidth (MHz)
v_V	Vehicle speed (km/h)
v_{max}	The maximum flying speed of UAVs (m/s)
P_U	Transmission power budget of each UAV (dBm)
$P_{i,j}^k$	Transmission power from the i-th UAV to the j-th vehicle on the k-th RB (dBm)
$g_{i,j}$	Channel gain between the i-th UAV and the j-th vehicle (dBm)
$\delta_{i,j}^k$	Assignment parameter of the j-th vehicle to the i-th UAV on the k-th RB
σ_w^2	Noise power (dBm)
P_{tol}	The minimum required power difference to perform SIC (dBm)
g_0	Channel gain at reference distance (dBm)
h_U	The flight altitude of UAVs (m)
L	The length of the road (Km)
d_{min}	The minimum distance between UAVs (m)

B. Paper Organization

This paper is organized as follows. Section II presents the system model, assumptions, and formulation of optimization problem for a multi-cell UAV-assisted vehicular communication network based on the NOMA system. In Section III, we present a two-phase suboptimal approach, which involves a user assignment algorithm in the initial phase, and Stackelberg game-based deployment design and resource allocation in the iteration phase, to effectively solve the main problem. The complexity analysis for the proposed algorithms is provided in Section IV. Section V delivers the simulation results to demonstrate the performance of the proposed solutions. Finally, concluding remarks are presented in Section VI.

II. System Model and Problem Formulation

In this section, we first describe the assumptions and details of the system model in Section II.A. Then, in Section II-B we formulate the main problem aiming to jointly achieve an efficient deployment design for UAVs and an optimal radio resource allocation for I2V links.

A list of notations used in this work is provided in Table I for the readers' reference.

A. System Model

As shown in Fig. 1, we consider a downlink vehicular communication network consisting of J vehicles, all equipped with omnidirectional antennas, traveling at speed v_V on a straight two-line road with a length of L km. Also, I UAVs, each one equipped with a directional antenna, fly at a maximum speed $v_{\max}$ at a fixed altitude h_U to support all vehicles on the road. A minimum distance between UAVs, denoted by $d_{\min}$, is considered to both avoid collisions and ensure coverage of the entire area.

In the proposed scenario, we assume that the Cartesian coordinates of vehicles are known a priory for a central entity, where the

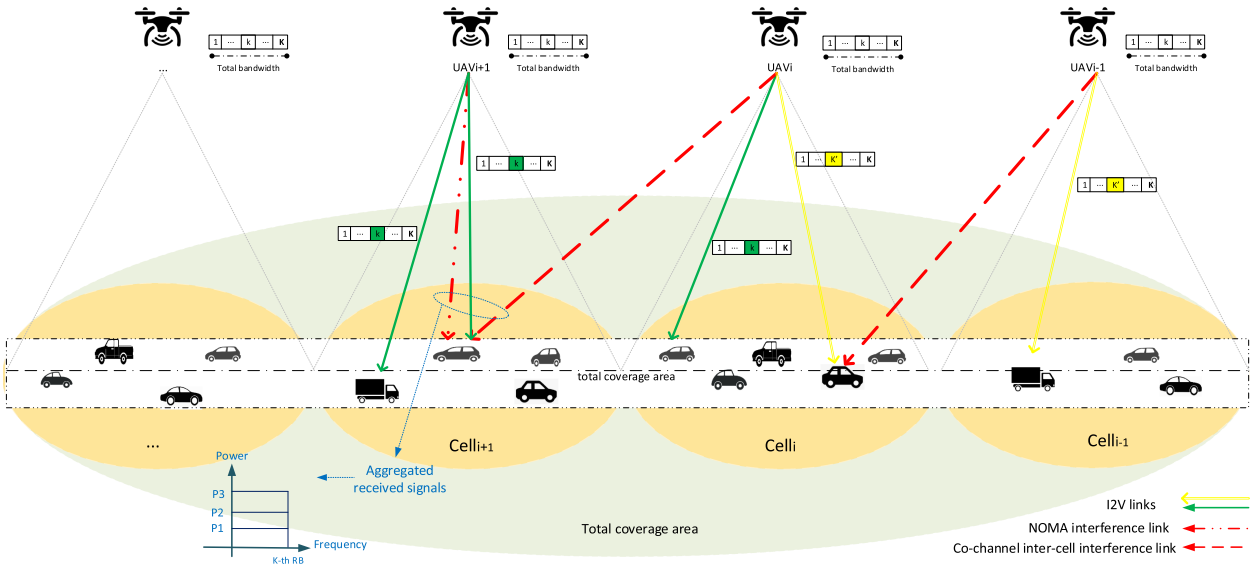

Fig. 1. Coordinated UAVs-assisted vehicular communication network, employing NOMA technique.

proposed algorithms are performed as offline phases. All UAVs remain connected to the central entity via wireless backhaul such as WiMax/millimeter-wave (mmW) and are aware of the locations of vehicles and the result of the proposed algorithms [7], [46].

Every UAV with a total power budget P_{U_i} and total available bandwidth B_T, is employed to serve a group of associated vehicles via air-to-ground (A2G) channels. All UAVs share the same frequency band with each other over consecutive time periods. The B_T is divided into K resource blocks (RBs), each one with the width of $\frac{B_T}{K}$. The UAV, vehicle, and resource block sets are denoted as $\mathcal{I} = \{1, 2, \ldots, I\}$, $\mathcal{J} = \{1, 2, \ldots, J\}$ and $\mathcal{K} = \{1, 2, \ldots, K\}$, respectively, where $|\mathcal{I}| = I$, $|\mathcal{J}| = J$, $|\mathcal{K}| = K$. Also, we use notations U_i and V_j to refer to the i-th UAV, and the j-th vehicle, and N_i expresses the total number of vehicles connected to UAV_i.

Let us consider that the total process time, T, is split into N_t equal time slots with the duration of $\Delta t = \frac{T}{N_t}$. We assume that the two-dimensional (2D) Cartesian coordinate of each vehicle V_j, is fixed at $Q_j = [x_j, y_j]^T \in R^{2\times 1}, j \in J$ within each time slot, but varies from one slot to another due to the vehicle's mobility. Considering all UAVs are flying at a fixed altitude h_U from the road surface, the time-varying 3D Cartesian coordinate of the i-th UAV at time instant $t, 0 \le t \le \Delta t$, can be expressed as $Q_i(t) = [x_i(t), y_i(t), h_U]^T \in R^{3\times 1}, i \in I$. Therefore, the Euclidean distance from the i-th UAV to the j-th vehicle over the k-th RB, at a time instant $t, 0 \le t \le \Delta t$, can be expressed as:

$$d_{i,j}(t) = ||Q_{U_i}(t) - Q_{V_j}|| = \left((x_i(t) - x_j)^2 + (y_i(t) - y_j)^2 + h_U^2\right)^{\frac{1}{2}}. \quad (1)$$

Furthermore, we assume that UAVs' displacement over each time slot is based on the velocity constraint as $||Q_{U_i}(t_n) - Q_{U_i}(t_n - 1)|| \le v_{\max}\Delta t, \forall t_n \in \{2, 3, \ldots, N_t\}$, which limits the maximum distance that each UAV can travel over a time slot.

To overcome the time-varying channel gain coefficients of traveling vehicles, Δt should be chosen small enough that the distances between UAVs and vehicles can be considered unchanged over each time slot, while they vary from one slot to another. Therefore, if we consider $v_{\max}\Delta t$ as the maximum allowed displacement of UAVs within each time slot, the required accuracy of the adopted Δt can be guaranteed by choosing a minimum N_t, as the following condition is satisfied [24]:

$$v_{\max}\Delta t \ll h_U \rightarrow N_t \ge \frac{v_{\max}T}{h_U\epsilon_t},$$

where ϵ_t is a predefined threshold for the ratio of the maximum UAV displacement within Δt and the flight altitude as $\frac{v_{\max}\Delta t}{h_U} \le \epsilon_t$. Although further increasing N_t enhances the accuracy, it also increases the complexity of design. Hence, N_t should be chosen properly to balance between complexity and accuracy.

For simplicity in the channel modeling, according to [45], and [24], we assume that there is no small-scale fading for the I2V links. It is also assumed that all I2V links are dominated by the LoS, and multi-path fading can be ignored [15]. Therefore, the I2V link quality mainly depends on the Euclidean distances from UAVs to the vehicles. Consequently, the channel gain from the i-th UAV to the j-th vehicle at the time moment t, corresponding to the free-space path loss model, can be expressed as [15], [24], [45], [47]:

$$g_{i,j}(t) = g_0 d_{i,j}^{-2}(t) = g_0\left((x_i(t) - x_j)^2 + (y_i(t) - y_j)^2 + h_U^2\right)^{-1} \quad (2)$$

where g_0 expresses the channel gain at the reference distance $d_0 = 1\ m$.

1) NOMA With SIC: We assume that the NOMA technique is applied for transmission in the studied multi-cell network in which J_K (as the NOMA factor) communication links in every cell share the same RB, simultaneously. Since in the NOMA, multiple users non-orthogonally access the same RB, a received signal on each RB is subject to the intra-cell interferences caused by co-channel and co-cell I2V links. Meanwhile, the inter-cell interferences caused by co-channel I2V links from the adjacent cells affect the received signal. Due to the strong interferences, each receiver performs SIC to recover its desired signal by successively canceling interferences based on differences in the transmission power domain [36]. Note that in the NOMA system, less power is allocated to the vehicle with higher channel gain, and more power is allocated to the vehicle with smaller

channel gain [33]. Subsequently, the SIC technique can be successfully carried out at the receivers with stronger channel gains to remove interference caused by vehicles with smaller channel gains. Hence, according to [32], a minimum power difference between the desired signal and interference signals, as a detection threshold P_{tol}, is required to SIC can successfully eliminate the interference and decode the desired signal. However, by applying SIC at the receiver of the j-th vehicle associated to the i-th UAV on the k-th RB, the interfering signal with the higher interference-cancellation order (ie $g_{i,j'} > g_{i,j}$), still remains as intra-cell interference, in addition to an inter-cell interference from the other UAVs transmission on same RBs. It is worth noting that while in [32] NOMA with SIC was studied in a single-cell scenario, the results are valid here. The reason is that although we investigate a multi-cell scenario, SIC is applied to each individual cell while inter-cell interference is treated the same as noise.

Note that we assumed that the channel gains remain unchanged within a time slot but vary from one slot to another due to vehicles' mobility. Hence, the order of the I2V channel gains change in terms of their strength and consequently their allocated power in different time slots. Therefore, the NOMA order of I2V links alters in different time slots.

Let us assume $\delta^k_{i,j}(t) = 1$ expresses that vehicle j is connected to the i-th UAV in resource block k, and $\delta^k_{i,j}(t) = 0$ if otherwise. Then, assume $x^k_{i,j}(t)$, the desired signal of the j-th I2V link user served by the i-th UAV on the k-th RB and at the moment t, is transmitted by the power budget of $P^k_{i,j}$. Therefore, the total achievable rate of the system over a time slot, in bits/second/Hertz (bps/Hz), can be formulated as follows:

$$R_{Total}(t) = \sum_{k=1}^{K}\sum_{i=1}^{I}\sum_{j=1}^{J}\delta^k_{i,j}\log\times \left(1+\frac{P^k_{i,j}(t)g_{i,j}(t)}{\sigma^2_w+\sum\limits_{i'=1\neq i}^{I}P^k_{U'_i}(t)g_{i',j}(t)+\sum\limits_{j'=1:g_{i,j'}>g_{i,j}}^{J}P^k_{i,j'}(t)g_{i,j}(t)}\right) \tag{3}$$

where σ^2_w indicates the AWGN noise power. The second phrase in the denominator of this equation, is the inter-cell interference caused by the other UAVs that transmit signals over the k-th RB. Also, the third phrase indicates the intra-cell interference caused by I2V links that non-orthogonally access the same RB, with the higher interference-cancellation order that can not be eliminated by SIC.

Finally, the average long-term achievable rate is computed as follows [39]:

$$\overline{R}(t) = \lim_{t\to\infty}\frac{1}{t}\sum_{\tau=1}^{t}R_{Total}(\tau). \tag{4}$$

B. Problem Formulation

Considering the system model details presented in Section II-A, a joint problem of user assignment, UAVs deployment design, and resource allocation is formulated with the aim of maximizing the data rate of I2V users in the presented scenario. We use notations of $A_i(t)$, $Q_{U_i}(t)$, $P^k_{i,j}(t)$, and $\delta^k_{i,j}(t)$ for the users' set assigned to the i-th UAV, the 3D position of the i-th UAV, the power and spectrum allocated to vehicles, respectively. Assuming a free-space path loss model for A2G channels, we arrange the I2V links' channel gains in descending order based on their distance [15]. Therefore, the optimizing problem can be formulated as:

$$\max_{\{Q_{U_i}(t)\},\{P^k_{i,j}(t)\},\{\delta^k_{i,j}(t)\},\{A_i(t)\}} \overline{R}(t)$$

$$\text{s.t.}\begin{cases} C5.1: \sum_{j=1}^{J}\sum_{k=1}^{K}\delta^k_{i,j}(t)P^k_{i,j}(t) \le P_{U_i},\ \forall i \\ C5.2: \sum_{j=1}^{J}\delta^k_{i,j}(t) \le J_K,\ \forall i,k \\ C5.3: \sum_{k=1}^{K}\delta^k_{i,j}(t) \le 1,\ \forall i,j \\ C5.4: \sum_{i=1}^{I}\sum_{k=1}^{K}\delta^k_{i,j}(t) \le 1,\ \forall j \\ C5.5: ||Q_{U_i}(t_n) - Q_{U_i}(t_n-1)|| \le v_{\max}\Delta t, \\ \quad \forall i, \forall t_n \in \{2,3,\ldots,N_t\} \\ C5.6: ||Q_{U_i}(t) - Q_{U'_i}(t)||^2 \ge d^2_{\min},\ \forall i \in \mathcal{I}, i' = i \pm 1 \\ C5.7: \left(\left(\delta^k_{i,j}(t)P^k_{i,j}(t) - \sum_{j'=1}^{j-1}\delta^k_{i,j'}(t)P^k_{i,j'}(t)\right)g_{i,j-1}(t)\right. \\ \left. -\sum_{i'=1\neq i}^{I}g_{i',j-1}(t)P^k_{U'_i}(t)\right) \ge P_{tol}, \forall k,i,\forall j=2,3,\ldots,J_K \\ C5.8: \delta^k_{i,j}(t) \in \{0,1\},\ \forall i,j,k \end{cases} \tag{5}$$

In this problem, Constraint $C5.1$ indicates the limitation of the total transmission power of every UAV. $C5.2$ states the NOMA constraint, where J_K users with different channel gains non-orthogonally share a spectrum resource block. $C5.3$ indicates that each I2V link can use at most one RB. $C5.4$ ensures that every vehicle can only connect to one UAV per time slot. $C5.5$ limits the horizontal distance that each UAV can travel over a time slot considering their maximum speed $v_{\max}$. Also, $C5.6$ ensures the collision avoidance of two adjacent UAVs and prevents their overlaps. $C5.7$ ensures the power difference constraint for efficient performing of SIC in a J_K-user NOMA cluster. $C5.8$ states that the user and spectrum assignment parameters can only be integer variables 0 or 1.

The optimization problem in (5) with jointly designing of vehicle-UAV association, power and spectrum allocation for a NOMA communication system, and UAVs deployment design has a combinatorial optimization nature. This problem involves both continuous and integer variables. Thus, it is an MINLP and solving such problem leads to an unreasonable high-complexity computation. To efficiently solve the optimization problem in (5), we propose a hierarchical approach in which we decompose the main problem into several low-complexity sub-problems and solve them in two successive phases. First, in an initial phase, we propose a low-complexity user assignment algorithm. Next, in an iteration phase, a Stackelberg game-based method is first presented to optimally design the UAVs positions. Then, the resource block assignment is obtained via an algorithmic approach. Finally, the transmission power allocation problem is presented, solved with KKT conditions, and the closed-form results are indicated.

A brief overview of the overall framework's operation is provided in Fig. 2 to show the connection between all the

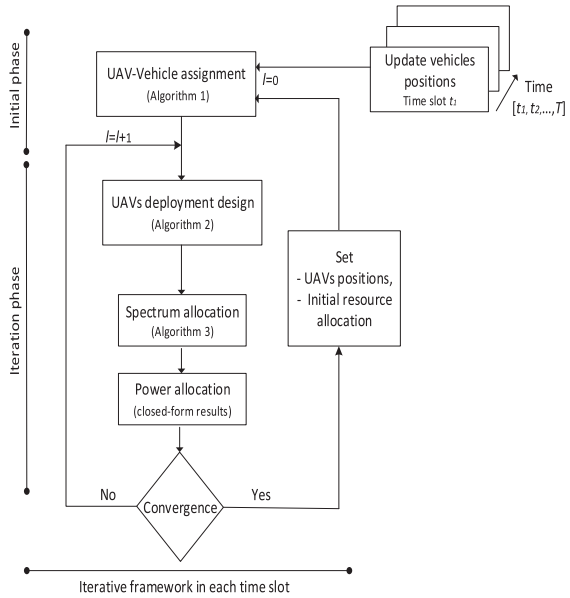

Fig. 2. General framework (Algorithm 4).

proposed algorithms. It can be seen that in the initial phase, at the beginning of each time slot, the optimal UAV-vehicle assignment is obtained by running Algorithm 1. In this phase, except in the first time slot (t_1), where the resources are allocated randomly, in other time slots they are allocated based on the optimal values obtained from the previous time slot. In the iteration phase, first, the optimum deployment of UAVs is designed via the Stackelberg game-based method depicted in Algorithm 2. Next, the optimal resource block assignment is obtained by running Algorithm 3. Then, the optimal power allocation is derived by solving an optimization problem that leads to closed-form results. This process continues in successive iterations for each time slot until convergence is reached and the overall near-optimal solution is obtained. Then, the achieved solutions are set as initial parameters for the next time slot. The presented hierarchical solution method is depicted in the overall Algorithm 4, while the details are presented in Section III.

In this work, we only focus on centralized algorithms. Our future work may study and evaluate a distributed algorithm for deployment design and resource allocation in such networks.

III. Proposed Solution for User Assignment, Deployment Design and Resource Allocation

In this section, we present the solution method in detail. Our proposed algorithm includes two main phases of initial and iteration for every time slot. First, in the initial phase, by proposing a user assignment algorithm, the formulated MINLP problem (5) is relaxed into deployment design and resource allocation. Next, in the iteration phase, we present solutions for both the optimum deployment design and resource allocation problems, and then we investigate results convergence.

A. Initial Phase

As depicted in Fig. 2, the optimal UAV-vehicle assignment is obtained in the initial phase and at the beginning of each time slot. After the user assignment, radio resources are allocated based on the optimal values obtained from the previous time slot. While in the first time slot (t_1), resources are allocated randomly.

Algorithm 1: UAV-Vehicle Assignment.

Inputs: $\{Q_{U_i}\}, \{Q_{V_j}\}, \mathcal{I} = \{1, 2, .., I\}, \mathcal{J} = \{1, 2, .., J\}, \mathcal{K} = \{1, 2, .., K\}, N_i = 0, \delta^k_{i,j} = 0 \forall i, j, k,$
Outputs: $\{A_i\} = \{\delta^k_{i,j}\}$.
1: **for** $i \in \mathcal{I}$, and $j \in \mathcal{J}$ **do**
2: Compute the $\{d_{i,j}\}$;
3: **end for**
4: **while** $\mathcal{J} = \{\}$, **do**
5: Find the $\arg(\min_j\{d_{i,j}\})$;
6: Assign j-th vehicle to the i-th UAV and set $\delta^k_{i,j} = 1$, for $k = 1, 2, \ldots, K$;
7: Set $N_i = N_i + 1$;
8: Set $\mathcal{J} = \mathcal{J} - \{j\}$;
9: **end while**
10: **End**.

1) UAV-Vehicle Association Algorithm: At the beginning of every time slot, considering the channel gains of I2V links, we assign all vehicles to UAVs via a UAV-vehicle association method depicted in Algorithm 1. Note that due to considering the channel gains corresponded to the free-space path loss model, it is preferred to sort the vehicles only based on their distances. Hence, in Algorithm 1, user assignment is mainly based on the vehicle-UAV distance in each time slot.

By performing this algorithm, the problem in (5) is relaxed into a joint problem of deployment design and resource allocation. To efficiently solve this problem, we run an iteration phase in which the deployment design and resource allocation problems are solved iteratively until convergence is achieved.

B. Iteration Phase

At the beginning of each iteration, the optimum deployment of UAVs is designed via the Stackelberg game-based method. Next, the optimal resource block assignment is obtained by a proposed algorithmic approach, and then, the optimal power allocation is derived via solving an optimization problem. In this phase, the optimal solution to each sub-problem is obtained by considering to be fixed the optimization parameters given from other sub-problems. This process continues in an iterative scheme until convergence is reached and the overall near-optimal solution is obtained. Therefore, by performing each iteration, l, the four hierarchical steps of deployment design, spectrum resource block assignment, power allocation, and convergence investigation are executed.

1) UAVs Deployment Design: At this step, the 2D positions of all UAVs are updated in order to both maximize the received power at the destinations and to minimize inter-cell interference. For simplicity, we assume that the interference effects of non-adjacent UAVs can be ignored. Note that due to large distance between UAVs, this assumption is reasonable. Therefore, each cell is affected by the inter-cell interferences from only two adjacent cells, and it seems that this cell competes with two adjacent cells for the highest sum rate.

Given the competitive nature of the above approach, we propose the Stackelberg game method for designing UAVs deployments. Hence, the Stackelberg game, consisting of a leader and followers that dynamically compete with each other to achieve more utility, is performed. In the proposed game, some UAVs act as leaders and others act as followers [48]. Since the utilities defined for the leader and follower groups are a function of the position of both groups, their movement affects each other's utility a lot. Therefore, the problems of both groups are solved dynamically until finding their optimal position. Without loss of generality, we assume that all UAVs are divided into three-member groups, with the middle UAV as the leader and the two side UAVs as the followers. Several necessary insights and assumptions to efficiently form the Stackelberg game are discussed below:

- The Stackelberg game as a competitive strategy to optimally update the UAVs' deployments is performed. All UAVs are categorized into the groups of leader and follower.
- According to this game, all UAVs compete to deliver the highest total power to associated users, while increasing transmission power increases inter-cell interference on other cells' users. Hence, for each UAV, we consider the total power received by the connected users as the utility function and the caused interference on other cells' users as the cost function.
- The game is run in N groups, where $N = [\frac{I+2}{3}]$ and I is the number of UAVs. In each group, three UAVs compete as Stackelberg game players. Thus, in the n-th group, where $n = 1, 2, 3, .., N$, the middle UAV (i.e., $\text{UAV}_{i=2n}$) acts as the leader, and side UAVs (i.e., $\text{UAV}_{i'=2n\pm1}$) act as the followers.
- In each group, the leader and followers find their position in competition with each other and in successive iterations until the convergence is achieved. First, the leader determines its position to obtain the maximum utility, and then according to this optimal point, the followers find their optimal positions to get their maximum utility [48].
- In the first group, the positions of both followers are unknown. While in the next groups, only one position (i.e., $\text{UAV}_{i'=2n+1}$) is unknown because one follower (i.e., $\text{UAV}_{i'=2n-1}$) found its position in the previous group.

Proof: Stackelberg equilibrium is proved in Appendix A. ■

Considering the unchanged position for vehicles over each time slot, the channel power gain in (2) is a function of the changes in the UAVs' 2D positions. Hence, in the n-th group, the utility function for the leader (UAV_i) can be written as a function of the UAVs' positions as follows:

$$U_{L_i} = \sum_{k=1}^{K}\left(\sum_{j=1}^{J}\delta_{i,j}^{k}P_{i,j}^{k}g_0(d_{i,j})^{-2} - \sum_{i'=i\pm1}\sum_{j'=1}^{J}\delta_{i',j'}^{k}P_{U_i}^{k} \times g_0(d_{i,j'})^{-2}\right) = \sum_{k=1}^{K}\left(\sum_{j=1}^{J}\delta_{i,j}^{k}\frac{P_{i,j}^{k}g_0}{||Q_{U_i}-Q_{V_j}||^2} - \sum_{i'=i\pm1}\sum_{j'=1}^{J}\delta_{i',j'}^{k}\frac{P_{U_i}^{k}g_0}{||Q_{U_i}-Q_{V_{j'}}||^2}\right) \tag{6}$$

where $i' = i \pm 1$ denotes the side UAVs. In Section II-A, after obtaining the user assignment parameters by running Algorithm 1, the coordinate range of i-th UAV is determined according to the nearest (i.e., $x_{i,\min}, y_{i,\min}$) and the farthest (i.e., $x_{i,\max}, y_{i,\max}$) connected vehicles. Thus, we should consider this issue as a constraint for the UAV coordinate range to guarantee that all associated vehicles remain within the coverage area over the current time slot. Now, the 2D position of the leader can be efficiently updated via the following optimization problem:

$$\max_{\{Q_{U_i}\}} U_{L_i}$$
$$\text{s.t.}\begin{cases} C7.1: ||Q_{U_i}(t_n) - Q_{U_i}(t_n-1)|| \le v_{\max}\Delta t, \\ \quad \forall t_n \in \{2,3,\ldots,N_t\} \\ C7.2: ||Q_{U_i} - Q_{U_i'}||^2 \ge d_{\min}^2,\ \forall i \in \mathcal{I}, i' = i \pm 1 \\ C7.3: x_{i,\min} \le x_i \le x_{i,\max}, y_{i,\min} \le y_i \le y_{i,\max} \end{cases} \tag{7}$$

where $C7.1$ limits the traveling distance over a time slot for UAVs. $C7.2$ ensures collision avoidance and $C7.3$ limits flying coordinate interval for UAVs to ensure that all associated vehicles remain connected to them. One can see that the utility function in its first term is non-concave with respect to Q_{U_i}. Also, the resulting set from Constraint $C7.2$ leads to the non-concavity of the problem. Hence, we propose some techniques to relax the problem into an alternative concave problem. First, Theorem 1 is given in the following in order to transform the first term in (6) into an equivalent concave alternative [49].

Theorem 1: Assume that we are searching for $Q_{U_i}^m$ as the UAV position at the current iteration m. Considering $Q_{U_i}^{m-1}$ as the given UAV position from the previous iteration, we have

$$\sum_{k=1}^{K}\sum_{j=1}^{J}\delta_{i,j}^{k}P_{i,j}^{k}g_0\frac{1}{||Q_{U_i}^{m}-Q_{V_j}||^2} \ge \sum_{k=1}^{K}\sum_{j=1}^{J}\delta_{i,j}^{k}P_{i,j}^{k}g_0\frac{2||Q_{U_i}^{m-1}-Q_{V_j}||^2 - ||Q_{U_i}^{m}-Q_{V_j}||^2}{\left(||Q_{U_i}^{m-1}-Q_{V_j}||^2\right)^2} \tag{8}$$

Proof: Since the function $\frac{a}{b+x}$ for any positive constants a and b, is convex with respect to x, it can be linearly approximated using the following inequality

$$\frac{a}{b+x} \ge \frac{a}{b+x_0} - \frac{a}{(b+x_0)^2}(x - x_0) \tag{9}$$

where x_0 is a given point. The Theorem 1 is proved by (9). ■

Besides, due to the non-convexity of the resulting set from Constraint $C7.2$, the problem still remains a non-concave optimization problem. Therefore, we utilize Lemma 1 to transform this constraint into a linear alternative.

Lemma 1: By applying the first-order Taylor expansion [24], [50] at a given local point $Q_{U_i}^{m-1}$ from the previous iteration, Constraint $C7.2$ can be lower-bounded and be transformed into a convex constraint with respect to $Q_{U_i}^{m}$ that refers to the 3D position of UAV_i at the current iteration m:

$$\left|\left|Q_{U_i}^{m} - Q_{U_{i'}}^{m-1}\right|\right|^2 \ge \left|\left|Q_{U_i}^{m-1} - Q_{U_{i'}}^{m-1}\right|\right|^2 + 2\left(Q_{U_i}^{m-1} - Q_{U_{i'}}^{m-1}\right)^T \left(Q_{U_i}^{m} - Q_{U_i}^{m-1}\right),\ \forall i \in \mathcal{I}, i' = i \pm 1 \tag{10}$$

where $Q_{U_i'}^{m-1}$ is the follower position which is found from the previous iteration. In order to verify Constraint $C7.2$, the right-hand side of (10) as the lower bound of adjacent UAVs' distances should be greater than $d_{\min}$. Therefore, this constraint converts to an approximate convex constraint with respect to $Q_{U_i}^m$.

As a result of Theorem 1 and Lemma 1, the problem in (7) at the m-th iteration, transforms into an alternative concave problem with respect to $Q_{U_i}^m$ as:

$$\max_{\left\{Q_{U_i}^m\right\}} \sum_{k=1}^{K}\left(\sum_{j=1}^{J}\delta_{i,j}^k P_{i,j}^k g_0 \frac{2||Q_{U_i}^{m-1}-Q_{V_j}||^2-||Q_{U_i}^m-Q_{V_j}||^2}{\left(||Q_{U_i}^{m-1}-Q_{V_j}||^2\right)^2} - \sum_{i'=i\pm1}\sum_{j'=1}^{J}\delta_{i',j'}^k \frac{P_{U_i}^k g_0}{||Q_{U_i}^m-Q_{V_{j'}}||^2}\right)$$

$$\text{s.t.}\begin{cases} C11.1: C7.1, C7.3 \\ C11.2: ||Q_{U_i}^{m-1}-Q_{U_{i'}}^{m-1}||^2+2\left(Q_{U_i}^{m-1}-Q_{U_{i'}}^{m-1}\right)^T \\ \left(Q_{U_i}^m-Q_{U_i}^{m-1}\right)\geq d_{\min}^2,\ \forall i\in\mathcal{I}, i'=i\pm1 \end{cases} \tag{11}$$

This concave problem can be solved in MATLAB by optimization solvers such as CVX toolbox that exploits the interior point method (IPM) to solve such optimization problem [51].

At this point, the utility function for the follower, considering the leader position obtained in the current iteration, can be represented as

$$U_{F_{i'}} = \sum_{i'=i\pm1}\sum_{k=1}^{K}\left(\sum_{j'=1}^{J}\delta_{i',j'}^k P_{i',j'}^k g_0 \left(d_{i',j'}\right)^{-2} - \sum_{j=1}^{J}\delta_{i,j}^k P_{i'}^k g_0 \times \left(d_{i',j}\right)^{-2}\right) = \sum_{i'=i\pm1}\sum_{k=1}^{K}\left(\sum_{j'=1}^{J}\delta_{i',j'}^k \frac{P_{i',j'}^k g_0}{||Q_{U_{i'}}-Q_{V_{j'}}||^2} - \sum_{j=1}^{J}\delta_{i,j}^k \frac{P_{U_{i'}}^k g_0}{||Q_{U_{i'}}-Q_{V_j}||^2}\right). \tag{12}$$

Through a similar process of transforming the leader problem into a concave alternative, the approximate linear problem of the follower case, at the m-th iteration, can be formulated as follows:

$$\max_{\{Q_{U_{i'}}^m\}} \sum_{i'=i\pm1}\sum_{k=1}^{K} \times\left(\sum_{j'=1}^{J}\delta_{i',j'}^k P_{i',j'}^k g_0 \frac{2||Q_{U_{i'}}^{m-1}-Q_{V_{j'}}||^2-||Q_{U_{i'}}^m-Q_{V_{j'}}||^2}{\left(||Q_{U_{i'}}^{m-1}-Q_{V_{j'}}||^2\right)^2} - \sum_{j=1}^{J}\delta_{i,j}^k \frac{P_{U_{i'}}^k g_0}{||Q_{U_{i'}}^m-Q_{V_j}||^2}\right)$$

$$\text{s.t.}\begin{cases} C13.1: ||Q_{U_{i'}}^m(t_n)-Q_{U_{i'}}^m(t_n-1)||\leq v_{\max}\Delta t, \\ \quad \forall t_n\in\{2,3,\ldots,N_t\}, i'=i\pm1 \\ C13.2: x_{i',\min}\leq x_{i'}\leq x_{i',\max}, y_{i',\min}\leq y_{i'}\leq y_{i',\max}, \\ \quad \forall i'=i\pm1 \\ C13.3: ||Q_{U_{i'}}^{m-1}-Q_{U_i}^m||^2+2\left(Q_{U_{i'}}^{m-1}-Q_{U_i}^m\right)^T \\ \left(Q_{U_{i'}}^m-Q_{U_{i'}}^{m-1}\right)\geq d_{\min}^2\ \forall i\in\mathcal{I}, i'=i\pm1 \end{cases} \tag{13}$$

Algorithm 2: UAVs Deployment Design (in the Loop l).

Inputs: $\mathcal{I},\mathcal{J},\mathcal{K},N,\{\delta_{i,j}^k\},\{P_{i,j}^k\},g_0,d_{\min},v_{\max},m=0$,
Outputs: $\{Q_{U_i}\}=\{x_i,y_i\},\forall i\in\mathcal{I}$

1: **for** $n=1:N$ **do**
2: Set $UAV_{i=2n}$ as leader, and $UAV_{i'=i\pm1}$ as follower;
3: Set $m=m+1$;
4: Solve the problem in (11) to obtain $Q_{U_i}^m$;
5: **if** $n=1$ **then**
6: Solve the problem in (13) to obtain $Q_{U_{i\pm1}}^m$;
7: **else**
8: Solve the problem in (13) to obtain $Q_{U_{i+1}}^m$;
9: **end if**
10: **if** $||Q_{U_i}^m-Q_{U_i}^{m-1}||\leq\epsilon_Q$ where, $0<\epsilon_Q\leq1$, **then**
11: Set $Q_{U_i}^*=Q_{U_i}^{m-1}$, and $Q_{U_{i\pm1}}^*=Q_{U_{i\pm1}}^{m-1}$;
12: **else**
13: Go to Step 3;
14: **end if**
15: **end for**
16: Compute all channel gains $\{g_{i,j}^{(l)}\}$;
17: **End**.

where $Q_{U_{i'}}^{m-1}$ is the follower position obtained in the previous iteration and $Q_{U_i}^m$ is the leader position obtained in the current iteration. As mentioned at the beginning of the section, in the first round, the optimal positions of the leader and two followers are found. While in other rounds, the position of follower $i'=i-1$ is obtained in the previous round, and we need to find the position of leader and follower $i'=i+1$. This approximate linear problem is efficiently solved by standard convex optimization solvers such as CVX that utilize IPM. The position update process is depicted in Algorithm 2 with all the details presented in this subsection.

In the following, according to the obtained optimal positions of the UAVs and the updated channel gains, we present efficient allocation schemes for radio resources.

2) Spectrum Resource Block Assignment: In this part, under any given associated user set and updated channel gains, we present a suboptimal resource block assignment scheme for NOMA-based vehicular communication. In this scheme, we assume that each cell is capable of using the whole frequency bandwidth. Then, exploiting channel power gain differences, the I2V links in each cell are categorized into clusters, where multiple users share the same resource block. This resource block is assigned to the cluster based on minimizing co-channel interference within the cluster. As a result, the spectrum efficiency enhances, and hence, the achievable sum rate of a considered cell increases. As depicted in Algorithm 3, we first determine the feasible number of clusters $\{NC_i\}$, then propose a suboptimal user grouping scheme, and finally, resource block assignment is performed.

By running this algorithm, according to resource allocation algorithms and clustering issues presented in [32], spectrum resource blocks are efficiently assigned to I2V user clusters in the current iteration (l) for each cell.

3) Transmission Power Allocation: At this point, we present a power allocation scheme for any given resource block cluster, in which users are sorted in descending order of channel gains. First, we express the total data rate in (bps/Hz) for UAV i, in

Algorithm 3: Clustering and Spectrum Resource Block Assignment (Considering a Universal Frequency Reuse Scenario, Where All UAVs' Cells Are Available to the Whole Bandwidth).

Inputs: $\{N_i\}, J_K, \mathcal{K}, \{g_{i,j}^{(l)}\}, \forall i$
Outputs: I2V links clusters $\{Cl_z\}, z = 1, 2, \ldots, NC_i$, with the assigned resource block k.

1: **for** $i \in \mathcal{I}$ **do**
2: Compute the number of clusters: $NC_i = [\frac{N_i}{J_K}] + \vartheta[N_i \mod J_K]$;
3: Sort I2V link users for each cell considering their descending channel gains: $V_{i,1}, V_{i,2}, ..., V_{i,j}, ..., V_{i,N_i}$, where $V_{i,x}$ implies x-th I2V link user associated to the i-th UAV;
4: Let $\mathcal{K} = \{1, 2, .., K\}$, $\mathcal{Z} = \{1, 2, .., NC_i\}$
5: **for** $z \in \mathcal{Z}$ **do**
$Cl_z = \{V_{i,z}, \vartheta[(J_K - 2)]V_{i,NC_i+z}, \vartheta[(J_K - 2)(J_K - 3)]V_{i,2NC_i+z}, ..., V_{i,N_i-(z-1)}\}$, where $\vartheta[x] = 0$ if $x = 0$, otherwise $\vartheta[x] = 1$;
6: Find the I2V user with the worst (smallest) channel gain in the cluster z and name it: j'_z;
7: **for** $k \in \mathcal{K}$ **do**
8: Compute the maximum NOMA interference at the receiver of j'_z-th I2V link, using

$$I^k_{Cl_z,max} = \sum_{j=1, j\in Cl_z}^{j'_z-1} g_{i,j'_z} P^k_{i,j};$$

9: **end for**
10: **end for**
11: Assign the k-th resource block to the z-th cluster where,

$$z = arg\left(\min_k I^k_{Cl_z,max}\right);$$

12: Set $\mathcal{K} = \mathcal{K} - \{k\}$;
13: Set $\mathcal{Z} = \mathcal{Z} - \{z\}$;
14: Go to Step 11;
15: **end for**
16: **End**.

resource block k as follows:

$$R^k_i = \sum_{j=1}^{J_k} log\left(1 + \frac{P^k_{i,j} g_{i,j}}{\sigma^2_w + \sum_{i'=i\pm1} P^k_{U_{i'}} g_{i',j} + \sum_{j'=1}^{j-1} P^k_{i,j'} g_{i,j}}\right) \quad (14)$$

where $P^k_{U_{i'}}$ denotes the total transmission power of UAV$_i$ over the k-th resource block. Then, the power allocation problem can be organized as follows:

$$\max_{\{P^k_{i,j}\}} R^k_i$$
$$\text{s.t.} \begin{cases} C15.1: \sum_{j=1}^{J_k} P^k_{i,j} \le P_{RB} \\ C15.2: \left(P^k_{i,j} - \sum_{j'=1}^{j-1} P^k_{i,j'}\right) g_{i,j-1} - \sum_{i'=i\pm1} g_{i',j-1} P^k_{U_{i'}} \\ \ge P_{tol},\ \forall j = 2, 3, \ldots, J_K \end{cases} \quad (15)$$

where Constraint $C15.1$ indicates the limitation of the total power of UAV$_i$ over the resource block k, and $C15.2$ ensures the SIC technique constraint. For this problem, the Lagrangian with multipliers λ and ν_j can be formulated as shown in (16) at the bottom of the page. Exploiting Karush-Kuhn-Tucker (KKT) conditions, results of (16) and numerical results of transmission power allocation for different $J_K = 2$, 3, 4 are presented in Appendix B and C, respectively.

In the following, the closed-form expressions of optimal power allocation for different I2V link users are derived:

$$P^{k*}_{i,1} = \frac{P_{RB}}{2^{J_K-1}} - \frac{P_{tol} + \sum_{i'=i\pm1} g_{i',J_K-1} P^k_{U_{i'}}}{2^{J_K-1} g_{i,J_K-1}} - \frac{P_{tol} + \sum_{i'=i\pm1} g_{i',J_K-2} P^k_{U_{i'}}}{2^{J_K-2} g_{i,J_K-2}} - \frac{P_{tol} + \sum_{i'=i\pm1} g_{i',J_K-3} P^k_{U_{i'}}}{2^{J_K-3} g_{i,J_K-3}} - \cdots - \frac{P_{tol} + \sum_{i'=i\pm1} g_{i',1} P^k_{U_{i'}}}{2 g_{i,1}}, \quad (17)$$

$$P^{k*}_{i,2} = \frac{P_{RB}}{2^{J_K-1}} - \frac{P_{tol} + \sum_{i'=i\pm1} g_{i',J_K-1} P^k_{U_{i'}}}{2^{J_K-1} g_{i,J_K-1}} - \frac{P_{tol} + \sum_{i'=i\pm1} g_{i',J_K-2} P^k_{U_{i'}}}{2^{J_K-2} g_{i,J_K-2}} - \frac{P_{tol} + \sum_{i'=i\pm1} g_{i',J_K-3} P^k_{U_{i'}}}{2^{J_K-3} g_{i,J_K-3}} - \cdots + \frac{P_{tol} + \sum_{i'=i\pm1} g_{i',1} P^k_{U_{i'}}}{2 g_{i,1}}, \quad (18)$$

$$P^{k*}_{i,j} = \frac{P_{RB}}{4} - \frac{P_{tol} + \sum_{i'=i\pm1} g_{i',j} P^k_{U_{i'}}}{4 g_{i,j}} + \frac{P_{tol} + \sum_{i'=i\pm1} g_{i',j-1} P^k_{U_{i'}}}{2 g_{i,j-1}}, \text{for} 3 \le j \le J_K - 1, \quad (19)$$

$$P^{k*}_{i,J_K} = \frac{P_{RB}}{2} + \frac{P_{tol} + \sum_{i'=i\pm1} g_{i',J_K-1} P^k_{U_{i'}}}{2 g_{i,J_K-1}}. \quad (20)$$

Proof: See Appendix B. ■

4) Convergence Investigation: The proposed iterative approach containing UAVs deployment design, resource block assignment, and power allocation terminates when convergence is achieved. Therefore, at the end of each iteration, the difference between the results of two consecutive iterations is calculated

$$\mathcal{L}(P^k_{i,j}, \lambda, \nu_j) = \sum_{j=1}^{J_K} log\left(1 + \frac{P^k_{i,j} g_{i,j}}{\sigma^2_{tot} + \sum_{i'=i\pm1} P^k_{U_{i'}} g_{i',j} + \sum_{j'=1}^{j-1} g_{i,j} P^k_{i,j'}}\right) - \lambda\left(\sum_{j=1}^{J_K} P^k_{i,j} - P_{RB}\right) + \sum_{j=2}^{J_K} \nu_j \left(g_{i,j-1} P^k_{i,j} - P_{tol} - \sum_{i'=i\pm1} g_{i',j-1} P^k_{U_{i'}} - \sum_{j'=1}^{j-1} g_{i,j-1} P^k_{i,j'}\right) \quad (16)$$

Algorithm 4: UAVs Deployment Design and I2V Radio Resource Allocation.

Inputs: $Q_{U_i}(t=0)=(x_{U_0},y_{U_0},h_U), i\in\mathcal{I}, Q_{V_j}(t)=(x_{V_j},y_{V_j},0), j\in\mathcal{J}$,
Outputs: $\{Q^*_{U_i}(t)\}, \{P^{k*}_{i,j}(t)\}, \{\delta^{k*}_{i,j}(t)\}$.
1: **for** $t=0:\Delta t:T$ **do**
2: Set $l=0$;
3: Assign all vehicles to UAVs based on Algorithm 1;
4: Allocate spectrum resource blocks to vehicles randomly;
5: Allocate transmission power to vehicles randomly;
6: Set $l=l+1$;
7: Update the position of all UAVs based on Algorithm 2;
8: Allocate spectrum resource blocks to vehicles based on Algorithm 3;
9: Allocate power to vehicles based on (17−20);
10: **if** $||\{P^{k(l)}_{i,j}\}-\{P^{k(l-1)}_{i,j}\}||\le\epsilon_P$ where, $0<\epsilon_P\le 1$, **then**
11: Set $Q^*_{U_i}(t)=Q^{(l)}_{U_i}(t)$, and $Q^*_{U_{i\pm1}}(t)=Q^{(l)}_{U_{i\pm1}}(t)$;
12: Set vehicles' new positions as $Q_{V_j}(t+\Delta t)=Q_{V_j}(t)+\Delta d, j\in\mathcal{J}$ where $\Delta d=\Delta t.v_V$;
13: Go to Step 1;
14: **else**
15: Go to Step 6;
16: **end if**
17: **end for**
18: **End**.

and compared with a predefined threshold, ϵ_P. If it is smaller than the threshold value, the convergence of the results is achieved and the positions obtained in this iteration are set as the optimal deployment of UAVs. The proposed process in this part is performed by:

$$||P^{k(l)}_{i,j}-P^{k(l-1)}_{i,j}||\le\epsilon_P\rightarrow P^{k*}_{i,j}=P^{k(l)}_{i,j}\rightarrow Q^*_{U_i}=Q^{(l)}_{U_i},\quad\forall i,j,k. \tag{21}$$

While the numerical results in Section V show that the proposed algorithm converges quickly after a few iterations, in some cases with high-density aerial or terrestrial networks, ensuring convergence may be more challenging. To overcome this challenge, we set the maximum allowed number of iterations for such cases where convergence may not occur within a time slot.

Finally, the overall scheme presented in this paper is depicted in Algorithm 4.

IV. Complexity Analysis

The computational complexity of the proposed scheme is discussed in this section. We also demonstrate that the proposed scheme leads to much lower computational complexity than an exhaustive search to solve the main problem. Let us assume that the proposed overall algorithm converges in L iterations. Therefore, the total complexity of the proposed scheme in each time slot can be organized as a linear function of the complexity of the main parts of Algorithm 4 as follows:

$$\varsigma=CX_{VU}+L(CX_{SG}+CX_{RB}+CX_P), \tag{22}$$

TABLE II
Computational Complexity Functions of Other Parts in the Proposed Scheme

Symbol	Computational complexity function
CX_{VU}	$\mathcal{O}(IJ)$
CX_{RB}	$\mathcal{O}(KIJ)$
CX_P	$\mathcal{O}(KIJ)$

where CX_{VU} refers to computational complexity of UAV-vehicle association, CX_{SG} is computational complexity of deployment design by Stackelberg game, CX_{RB} states resource block assignment complexity, and CX_P refers to power allocation complexity.

Since we derived closed-form expressions for power allocation and presented low-complexity algorithms for users and resource block assignment, the major computational complexity of the overall algorithm comes from the deployment design for UAVs. This part of Algorithm 4 is an iterative approach running in subloops and includes two deployment design subproblems for leader and follower in (11) and (13). Therefore, if these subproblems converge in M iterations, the complexity of performing the Stackelberg game for deployment design can be derived as follows:

$$CX_{SG}=M(R_1+R_2), \tag{23}$$

where R_1 and R_2 are computational complexity of (11) and (13) which are solved via CVX toolbox. Note that when problem x is solved via CVX that employs IPM, the computational complexity is $R_x=\frac{\log(\frac{A_x}{\eta_0\xi})}{\log(\partial)}$, where A_x is the number of constraints of problem x, η_0 refers to an initial point for approximating the accuracy of IPM, $\xi\in(0,1]$ indicates a criterion to stop IPM, and ∂ is utilized to update the accuracy of IPM [51], [52]. Hence, R_1 and R_2 can be derived as follows:

$$R_1=\begin{cases}\frac{\log\left(\frac{2}{\eta_0\xi}\right)}{\log(\partial)}, & \text{if } I \text{ is even}\\ \frac{\log\left(\frac{3}{\eta_0\xi}\right)}{\log(\partial)}, & \text{if } I \text{ is odd}\end{cases} \tag{24}$$

and

$$R_2=\begin{cases}\frac{2\log\left(\frac{4}{\eta_0\xi}\right)+(I-2)\log\left(\frac{2}{\eta_0\xi}\right)}{\log(\partial)}, & \text{if } I \text{ is even}\\ \frac{2\log\left(\frac{5}{\eta_0\xi}\right)+(I-2)\log\left(\frac{2}{\eta_0\xi}\right)}{\log(\partial)}, & \text{if } I \text{ is odd}\end{cases} \tag{25}$$

By replacing R_1 and R_2 in (23), the main complexity of the proposed scheme that comes from the deployment design is obtained. The complexity of other parts of Algorithm 4 is summarized in Table II [53]. Therefore, the total complexity of the proposed suboptimal scheme can be obtained from (22), which is much lower than the computational complexity originating from solving the main problem in (5). The reason is that the computational complexity of the exhaustive search for solving the main problem in (5) is obtained by an exponential function of multiplication of the number of UAVs, I, number of vehicles, J, number of resource blocks, K, and possible solutions of transmission power and UAVs positions. In this exhaustive search solution, for each time slot, all possible solutions for UAVs positions, user assignment, and resource allocations are investigated in order to satisfy all constraints in (5). Subsequently, among the feasible solutions, we should search for the optimum

TABLE III
PREDEFINED PARAMETERS FOR SIMULATIONS

Simulation parameter	Value
Number of users	70
Number of UAVs	5
Number of resource blocks (RBs)	16
Number of co-channel users (NOMA factor)	2
Length of the road	1000 m
Vehicle speed	60 km/h
Maximum transmission power of UAVs	40 dBm
Noise power	-100 dBm
Minimum power difference to perform SIC	-120 dBm
Channel gain at reference distance	-50 dBm
Time duration	30 sec
Size of each time slot	1 sec
Flight altitude of UAVs	14 m
Minimum distance between UAVs	50 m

solution corresponding to the maximum objective function in (5). Hence, the exhaustive search solution leads to a much higher computational complexity than the proposed algorithms.

V. NUMERICAL EVALUATION

In this section, simulation results are presented to demonstrate the effectiveness of the proposed deployment design and radio resource allocation. First, we refer to assumptions and predefined parameters in Subsection A, and then the obtained simulation results are evaluated in Subsection B.

A. Simulation Assumptions

Following the presented details in Section II, we consider a suburban environment as the proposed system platform, where 5 UAVs are deployed at a fixed altitude and a flight mode with a maximum speed of 10 m/s to support offloading or temporary traffic of the vehicular communication network. The served vehicles travel along a two-lane road in parallel, with a fixed speed of 60 km/h. Also, we mentioned in Section II that all I2V channels are dominated by LoS links and thus multipath fading is ignored.

A summary of the predefined parameters for the simulation is presented in Table III.

B. Simulation Results

In this section, we investigate the performance of the proposed scheme through simulation. For a fair evaluation, we consider three specific benchmark schemes of multi-UAV-assisted vehicular networks: (a) OMA system, which in contrast with the NOMA, every resource block is exclusively allocated to a single I2V link; (b) Static mode, which in contrast with the dynamic mode, the UAVs are assumed to be fixed; (c) Successive convex approximation (SCA) programming, which instead of the proposed game, the non-convex problem is transformed into the approximated convex problem [52].

Numerical results demonstrate the effectiveness of the proposed scheme using NOMA along with the Stackelberg game in dynamic mode. Simulations are carried out via MATLAB using a computer with Intel(R) Core(TM) i5-6200 U CPU 64-bit and 8 GB RAM.

Fig. 3 illustrates the I2V average sum-rate curves versus the UAVs flying altitude changes. It is assumed that in this range of altitude changes, the coverage area of all UAVs still remains

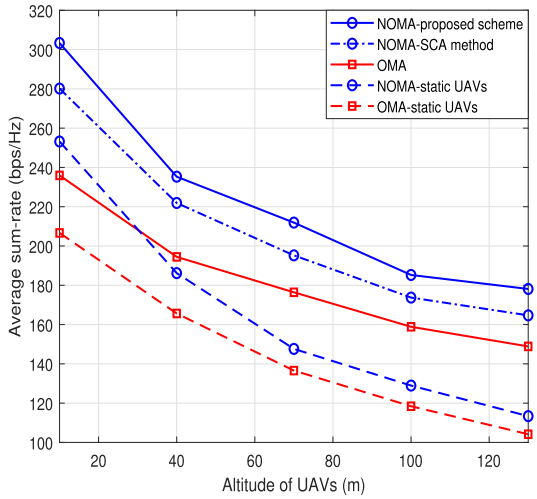

Fig. 3. Average sum-rate of I2V links versus flight altitude of UAVs for the proposed scheme, static mode, SCA method, and OMA.

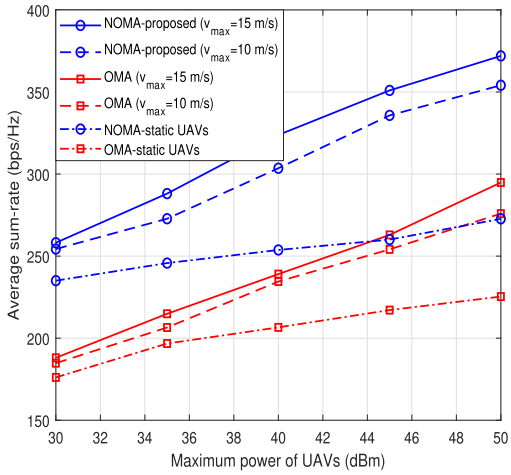

Fig. 4. Average sum-rate of I2V links versus maximum UAVs transmission power for proposed scheme, static mode, and OMA, for different values of $v_{\max}$.

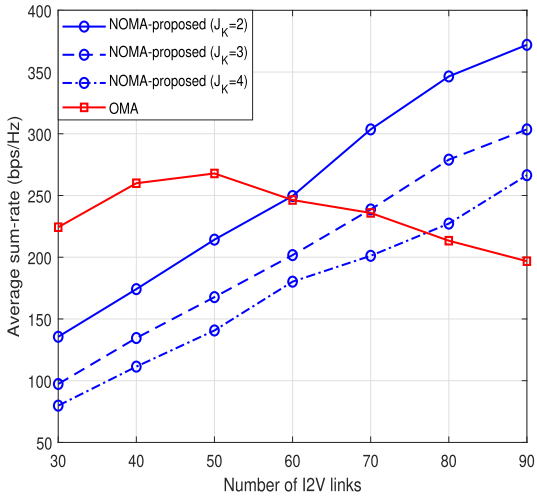

Fig. 5. Average sum-rate of I2V links versus total number of I2V links users, J, in the proposed scheme with different values of J_K and OMA.

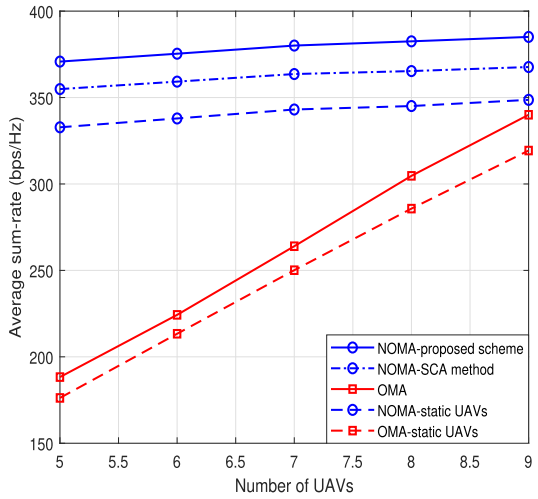

Fig. 6. Average sum-rate of I2V links versus number of UAVs, I, for the proposed scheme, static mode, SCA method, and OMA, when $J = 100$ and $d_{\min} = 25\,m$.

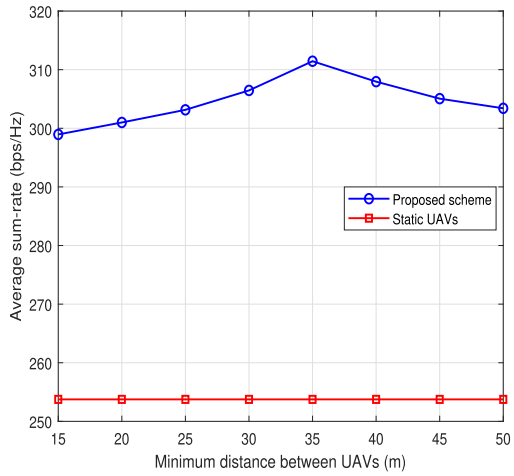

Fig. 7. Average sum-rate of I2V links versus minimum distance between UAVs, $d_{\min}$, for the proposed scheme and static mode.

unchanged. According to the system model presented in Section II, the I2V channels from UAVs to vehicles are dominated by LoS. Hence, when the flight altitude of UAVs increases and thus the Euclidean distance increases, the I2V channel coefficients decrease. Therefore, with increasing altitude, the achievable rate of I2V links decreases for all cases of the proposed scheme, SCA method, static mode, and OMA. Meanwhile, in the proposed scheme along with NOMA while $J_K = 2$, more efficiency is observed than in the other cases. Also, the proposed cooperative mode of UAVs is more efficient in terms of sum rate than the static mode where all UAVs are considered as static aerial BSs.

Fig. 4 reveals the effectiveness of the proposed scheme with dynamic mode at the maximum allowed flight speed, $v_{\max} = 15\ m/s$. To justify the effect of UAV speed on the sum rate, one reason is that as the speed increases, the capability of the UAV to adjust its optimal position enhances, hence the system sum rate is improved. Furthermore, this figure depicts the advantage of the NOMA technique with $J_K = 2$ over OMA. Besides, it is obvious that as the UAV transmission power budget increases, the achievable sum-rate increases for both cases of dynamic and static modes along with NOMA and OMA. Meanwhile, in static cases with no changes in UAVs' positions, there is less sensitivity to the increase in transmission power.

Fig. 5 depicts the average sum-rate versus the number of I2V users in the proposed scheme with different values of $J_K = 2$, 3, and 4, and OMA. While a strong advantage of NOMA methods is shown especially in cases with more users demanding I2V links, it can be observed that the highest average sum-rate is obtained in the case of $J_K = 2$. We also expect the system sum-rate to increase as the number of I2V link users increases until all resource blocks in all cells are employed by more than J_K users. After that, the sum rate for NOMA curves is descending due to increasing interferences. While in the OMA case, when the number of users exceeds 50, the sum rate reaches its maximum value and then decreases. The reason is that there are no more unused resource blocks to allocate orthogonally to I2V users.

Fig. 6 illustrates the impact of the number of UAVs on the users' sum rate in the proposed scheme, SCA method, static mode, and OMA. It can be seen that the performance of OMA systems improves as the number of UAVs, I, increases, while NOMA systems are less sensitive to the increase of I. One can justify that as I increases, there are more cells with fewer users, and as a result, there is no need to share a resource block among multiple users. Therefore, with the increase of I to more than 5, the sum rate in the OMA system enhances more than in the NOMA systems. Overall, the advantage of the proposed scheme is observed in terms of the sum rate compared to other benchmark schemes.

In Fig. 7, the average sum-rate curves of both the proposed method and the static mode of UAVs with the change of the minimum distance between adjacent UAVs are shown. One can see that in the proposed scheme, increasing the minimum distance leads to an increase in the system sum-rate until $d_{\min} = 35\ m$, after which the sum rate decreases. This is not far-fetched, because, with a large increase in $d_{\min}$, fewer UAVs cooperate to support the network. While the static mode is not sensitive to changes in $d_{\min}$. Also, the advantage of the proposed scheme is strongly demonstrated in terms of the average sum-rate.

Fig. 8 is given to evaluate the convergence behavior of the proposed scheme under different values of (a) number of I2V links, $J = 40$, 60, and 70, (b) maximum UAV transmission power, $P_U = 30$, 40, and 50 dBm, (c) initial random or fixed values. The results show that the proposed algorithm for all cases only needs several iterations to converge. This indicates that the proposed algorithm is computationally efficient and has a fast convergence rate. Meanwhile, one can see from Fig. 8(a) that the speed of convergence slows down slightly as the number of I2V links increases. The reason is that the computational complexity increases with the increase of users according to the complexity analysis presented in Section IV. While it can be seen from Fig. 8(b) that the change in the transmission power of UAVs does not change the convergence speed. This is because the computational complexity of the proposed algorithm is not much sensitive to the transmission power. Furthermore, as can be seen from Fig. 8(c), there is no major improvement or degradation in convergence when the resources are randomly allocated or considered as fixed values in the initial phase in the first time slot.

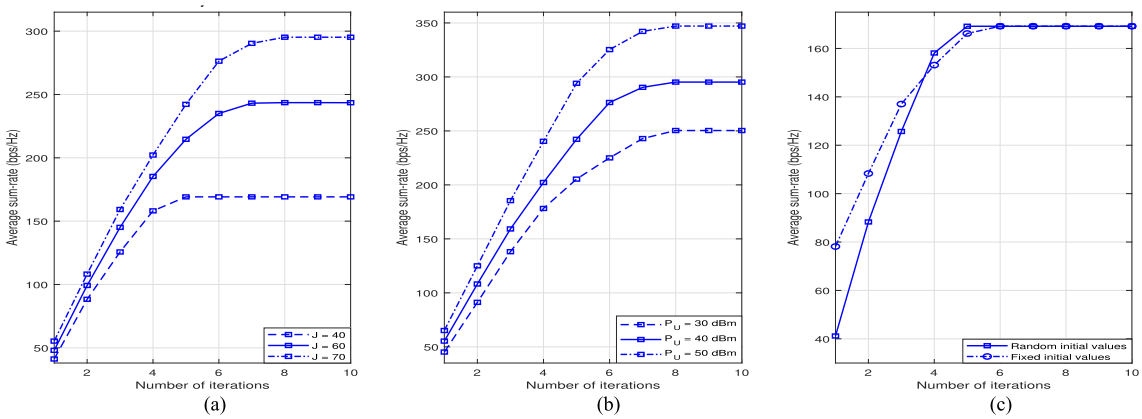

Fig. 8. Convergence behavior of the proposed algorithm in one time slot, under different parameters of (a) number of I2V links, (b) maximum transmission power of UAVs, (c) initial random\fixed values.

TABLE IV
COMPUTATIONAL COMPLEXITY VS. DIFFERENT SYSTEM SETUP

	J=40	J=50	J=60	J=70
I=3	170.6 sec	192.1 sec	205.2 sec	218.4 sec
I=5	190.2 sec	208.5 sec	224.1 sec	247.6 sec

The computational complexity under different parameters, the number of UAVs, I, and the number of I2V links, J, is given in Table IV. It can be seen from Table IV that the required run time of the proposed algorithm increases with the increase in the number of UAVs and the number of I2V links. This is also verified by the complexity analysis in Section IV. Furthermore, one can see that the impact of the number of UAVs on the run time is more than the number of I2V links. However, it can be seen that the proposed algorithm is computationally efficient for a moderate system setup.

VI. CONCLUSION

In this paper, we investigated the deployment design and resource allocation in a coordinated UAVs-assisted vehicular communication network, where flying UAVs support the connectivity of moving vehicles. To efficiently design the deployment of UAVs, we proposed a Stackelberg game-based technique where UAVs compete with each other to serve their associated vehicles at the highest achievable rate. Also, we applied the NOMA technique with SIC to obtain high efficiency in radio resource allocation, then we exploited a low-complexity spectrum assignment algorithm and obtained closed-form expressions for power allocation. Simulation results demonstrated the fast convergence and effectiveness of the proposed scheme along with the Stackelberg game and NOMA.

APPENDIX A

Let us assume that U_L and U_F are utility functions of the leader and followers with the optimum results of α^* and β^*, respectively. If the following inequalities are satisfied for any results α and β, then α^* and β^* are Stackelberg equilibrium points [43], [48]

$$U_L(\alpha^*, \beta^*) \geq U_L(\alpha, \beta^*)$$

and,

$$U_F(\alpha^*, \beta^*) \geq U_F(\alpha^*, \beta).$$

In the proposed Stackelberg game, the leader chooses the best response to optimize its utility considering the observed response of the follower. Then, the follower chooses its best response to optimize its utility based on the obtained leader's response. This process runs in consecutive iterations until the responses converge to the Stackelberg equilibrium point (α^*, β^*). In this case, the optimum result of the leader (α^*) does not change anymore with the obtained optimum result of the follower (β^*).

APPENDIX B

Considering the KKT conditions for equation (16), we have:

$$\frac{\partial \mathcal{L}}{\partial P_{i,1}^{k*}} = \frac{g_{i,1}}{\sigma_{tot}^2 + \sum_{i'=i\pm1} g_{i',1} P_{U_{i'}}^k + P_{i,1}^k g_{i,1}} - \sum_{x=2}^{J_K} \frac{\mathcal{A}}{\mathcal{B}.\mathcal{C}} - \lambda - \sum_{j'=2}^{J_K} \nu_{j'} g_{i,j'-1}^k \leq 0, \quad if \quad P_{i,1}^{k*} \geq 0 \tag{26}$$

and,

$$\frac{\partial \mathcal{L}}{\partial P_{i,j}^{k*}} = \frac{g_{i,j}}{\sigma_{tot}^2 + \sum_{i'=i\pm1} g_{i',j} P_{U_{i'}}^k + \sum_{j'=1}^{j-1} P_{i,j'}^k g_{i,j}} - \sum_{x=j+1}^{J_K} \frac{\mathcal{A}}{\mathcal{B}.\mathcal{C}} - \lambda - \sum_{j'=j+1}^{J_K} \nu_{j'} g_{i,j'-1} \leq 0, \quad if \quad P_{i,j}^{k*} \geq 0 \tag{27}$$

where,

$$\mathcal{A} = P_{i,x}^k (g_{i,x})^2$$

$$\mathcal{B} = \left(\sigma_{tot}^2 + \sum_{i'=i\pm1} g_{i',j} P_{U_{i'}}^k + \sum_{l=1}^{x} g_{i,x} P_{i,l}^k \right)$$

$$\mathcal{C} = \left(\sigma_{tot}^2 + \sum_{i'=i\pm1} g_{i',j} P_{U_{i'}}^k + \sum_{l'=1}^{x-1} g_{i,x} P_{i,l'}^k \right).$$

Also,

$$\frac{\partial \mathcal{L}}{\partial \lambda^*} = -\sum_{j=1}^{J_K} P_{i,j}^k + P_{RB} \geq 0, \quad if \quad \lambda^* \geq 0 \tag{28}$$

and,

$$\frac{\partial \mathcal{L}}{\partial \nu_j^*} = g_{i,j-1} P_{i,j}^k - \sum_{j'=1}^{j-1} g_{i,j-1} P_{i,j'}^k - \sum_{i'=i\pm 1} g_{i',j} P_{U_{i'}}^k - P_{tol} \geq 0, \quad if \quad \nu_j^* \geq 0, \quad \forall j = 2, 3, .., J_K. \tag{29}$$

APPENDIX C

The numerical results of power allocation for different values of $J_K = 2$, 3, and 4 from problem in (15), are obtaind as:

$\boldsymbol{J_K = 2}, (\lambda^*, \nu_2^*)$:

$$P_{i,1}^{k*} = \frac{P_{RB}}{2} - \frac{P_{tol} + \sum_{i'=i\pm 1} g_{i',1} P_{U_{i'}}^k}{2 g_{i,1}},$$

$$P_{i,2}^{k*} = \frac{P_{RB}}{2} + \frac{P_{tol} + \sum_{i'=i\pm 1} g_{i',1} P_{U_{i'}}^k}{2 g_{i,1}}.$$

$\boldsymbol{J_K = 3}, (\lambda^*, \nu_2^*, \nu_3^*)$:

$$P_{i,1}^{k*} = \frac{P_{RB}}{4} - \frac{P_{tol} + \sum_{i'=i\pm 1} g_{i',2} P_{U_{i'}}^k}{4 g_{i,2}} - \frac{P_{tol} + \sum_{i'=i\pm 1} g_{i',1} P_{U_{i'}}^k}{2 g_{i,1}},$$

$$P_{i,2}^{k*} = \frac{P_{RB}}{4} - \frac{P_{tol} + \sum_{i'=i\pm 1} g_{i',2} P_{U_{i'}}^k}{4 g_{i,2}} + \frac{P_{tol} + \sum_{i'=i\pm 1} g_{i',1} P_{U_{i'}}^k}{2 g_{i,1}},$$

$$P_{i,3}^{k*} = \frac{P_{RB}}{2} + \frac{P_{tol} + \sum_{i'=i\pm 1} g_{i',2} P_{U_{i'}}^k}{2 g_{i,2}}.$$

$\boldsymbol{J_K = 4}, (\lambda^*, \nu_2^*, \nu_3^*, \nu_4^*)$:

$$P_{i,1}^{k*} = \frac{P_{RB}}{8} - \frac{P_{tol} + \sum_{i'=i\pm 1} g_{i',3} P_{U_{i'}}^k}{8 g_{i,3}} - \frac{P_{tol} + \sum_{i'=i\pm 1} g_{i',2} P_{U_{i'}}^k}{4 g_{i,2}} - \frac{P_{tol} + \sum_{i'=i\pm 1} g_{i',1} P_{U_{i'}}^k}{2 g_{i,1}},$$

$$P_{i,2}^{k*} = \frac{P_{RB}}{8} - \frac{P_{tol} + \sum_{i'=i\pm 1} g_{i',3} P_{U_{i'}}^k}{8 g_{i,3}} - \frac{P_{tol} + \sum_{i'=i\pm 1} g_{i',2} P_{U_{i'}}^k}{4 g_{i,2}} + \frac{P_{tol} + \sum_{i'=i\pm 1} g_{i',2} P_{U_{i'}}^k}{2 g_{i,1}},$$

$$P_{i,3}^{k*} = \frac{P_{RB}}{4} - \frac{P_{tol} + \sum_{i'=i\pm 1} g_{i',3} P_{U_{i'}}^k}{4 g_{i,3}} + \frac{P_{tol} + \sum_{i'=i\pm 1} g_{i',2} P_{U_{i'}}^k}{2 g_{i,2}},$$

$$P_{i,4}^{k*} = \frac{P_{RB}}{2} + \frac{P_{tol} + \sum_{i'=i\pm 1} g_{i',3} P_{U_{i'}}^k}{2 g_{i,3}}. \tag{30}$$

REFERENCES

[1] E. Ahmed and H. Gharavi, "Cooperative vehicular networking: A survey," *IEEE Trans. Intell. Transp. Syst.*, vol. 19, no. 3, pp. 996–1014, Mar. 2018.

[2] S. Ilarri, T. Delot, and R. Trillo-Lado, "A data management perspective on vehicular networks," *IEEE Commun. Surveys Tuts.*, vol. 17, no. 4, pp. 2420–2460, Oct.–Dec. 2015.

[3] L. P. Qian, Y. Wu, H. Zhou, and X. Shen, "Non-orthogonal multiple access vehicular small cell networks: Architecture and solution," *IEEE Netw.*, vol. 31, no. 4, pp. 15–21, Jul./Aug. 2017.

[4] Y. Han, E. Ekici, H. Kremo, and O. Altintas, "Throughput-efficient channel allocation algorithms in multi-channel cognitive vehicular networks," *IEEE Trans. Wireless Commun.*, vol. 16, no. 2, pp. 757–770, Feb. 2017.

[5] X. Zhu, Y. Li, D. Jin, and J. Lu, "Contact-aware optimal resource allocation for mobile data offloading in opportunistic vehicular networks," *IEEE Trans. Veh. Technol.*, vol. 66, no. 8, pp. 7384–7399, Aug. 2017.

[6] W. Quan, M. Liu, N. Cheng, X. Zhang, D. Gao, and H. Zhang, "Cybertwin-driven DRL-based adaptive transmission scheduling for software defined vehicular networks," *IEEE Trans. Veh. Technol.*, vol. 71, no. 5, pp. 4607–4619, May 2022.

[7] M. Patra, R. Thakur, and C. S. R. Murthy, "Improving delay and energy efficiency of vehicular networks using mobile femto access points," *IEEE Trans. Veh. Technol.*, vol. 66, no. 2, pp. 1496–1505, Feb. 2017.

[8] N. Cheng et al., "A comprehensive simulation platform for space-air-ground integrated network," *IEEE Wireless Commun.*, vol. 27, no. 1, pp. 178–185, Feb. 2020.

[9] Y. Zeng, R. Zhang, and T. J. Lim, "Wireless communications with unmanned aerial vehicles: Opportunities and challenges," *IEEE Commun. Mag.*, vol. 54, no. 5, pp. 36–42, May 2016.

[10] M. Mozaffari, W. Saad, M. Bennis, Y.-H. Nam, and M. Debbah, "A tutorial on UAVs for wireless networks: Applications, challenges, and open problems," *IEEE Commun. Surveys Tuts.*, vol. 21, no. 3, pp. 2334–2360, Jul.–Sep. 2019.

[11] X. Mu, Y. Liu, L. Guo, J. Lin, and H. V. Poor, "Intelligent reflecting surface enhanced multi-UAV NOMA networks," *IEEE J. Sel. Areas Commun.*, vol. 39, no. 10, pp. 3051–3066, Oct. 2021.

[12] Y. Wu, J. Xu, L. Qiu, and R. Zhang, "Capacity of UAV-enabled multicast channel: Joint trajectory design and power allocation," in *Proc. IEEE Int. Conf. Commun.*, 2018, pp. 1–7.

[13] M. Samir, M. Chraiti, C. Assi, and A. Ghrayeb, "Joint optimization of UAV trajectory and radio resource allocation for drive-thru vehicular networks," in *Proc. IEEE Wireless Commun. Netw. Conf.*, 2019, pp. 1–6.

[14] L. Deng, G. Wu, J. Fu, Y. Zhang, and Y. Yang, "Joint resource allocation and trajectory control for UAV-enabled vehicular communications," *IEEE Access*, vol. 7, pp. 132806–132815, 2019.

[15] O. Abbasi, H. Yanikomeroglu, A. Ebrahimi, and N. M. Yamchi, "Trajectory design and power allocation for drone-assisted NR-V2X network with dynamic NOMA/OMA," *IEEE Trans. Wireless Commun.*, vol. 19, no. 11, pp. 7153–7168, Nov. 2020.

[16] Y. He, D. Wang, F. Huang, R. Zhang, and J. Pan, "Trajectory optimization and channel allocation for delay sensitive secure transmission in UAV-relayed VANETs," *IEEE Trans. Veh. Technol.*, vol. 71, no. 4, pp. 4512–4517, Apr. 2022.

[17] A. Al-Hourani, S. Kandeepan, and A. Jamalipour, "Modeling air-to-ground path loss for low altitude platforms in urban environments," in *Proc. IEEE Glob. Commun. Conf.*, 2014, pp. 2898–2904.

[18] S. Sekander, H. Tabassum, and E. Hossain, "Multi-tier drone architecture for 5G/B5G cellular networks: Challenges, trends, and prospects," *IEEE Commun. Mag.*, vol. 56, no. 3, pp. 96–103, Mar. 2018.

[19] Y. Zhou, N. Cheng, N. Lu, and X. S. Shen, "Multi-UAV-aided networks: Aerial-ground cooperative vehicular networking architecture," *IEEE Veh. Technol. Mag.*, vol. 10, no. 4, pp. 36–44, Dec. 2015.

[20] W. Fawaz, R. Atallah, C. Assi, and M. Khabbaz, "Unmanned aerial vehicles as store-carry-forward nodes for vehicular networks," *IEEE Access*, vol. 5, pp. 23710–23718, 2017.

[21] L. Gupta, R. Jain, and G. Vaszkun, "Survey of important issues in UAV communication networks," *IEEE Commun. Surveys Tuts.*, vol. 18, no. 2, pp. 1123–1152, Apr.–Jun. 2016.

[22] J. Wang et al., "Multiple unmanned-aerial-vehicles deployment and user pairing for nonorthogonal multiple access schemes," *IEEE Internet Things J.*, vol. 8, no. 3, pp. 1883–1895, Feb. 2021.

[23] J.-H. Chiu, Y.-C. Kuo, J.-P. Sheu, and Y.-W. P. Hong, "Energy-efficient UAV deployment and IoT device association in fixed-wing multi-UAV networks," in *Proc. IEEE Glob. Commun. Conf.*, 2020, pp. 1–6.

[24] Q. Wu, Y. Zeng, and R. Zhang, "Joint trajectory and communication design for multi-UAV enabled wireless networks," *IEEE Trans. Wireless Commun.*, vol. 17, no. 3, pp. 2109–2121, Mar. 2018.
[25] L. Dai, B. Wang, Y. Yuan, S. Han, I. Chih-Lin, and Z. Wang, "Non-orthogonal multiple access for 5G: Solutions, challenges, opportunities, and future research trends," *IEEE Commun. Mag.*, vol. 53, no. 9, pp. 74–81, Sep. 2015.
[26] H. Zhang, F. Fang, J. Cheng, K. Long, W. Wang, and V. C. Leung, "Energy-efficient resource allocation in NOMA heterogeneous networks," *IEEE Wireless Commun.*, vol. 25, no. 2, pp. 48–53, Apr. 2018.
[27] W. Ni, X. Liu, Y. Liu, H. Tian, and Y. Chen, "Resource allocation for multi-cell IRS-aided NOMA networks," *IEEE Trans. Wireless Commun.*, vol. 20, no. 7, pp. 4253–4268, Jul. 2021.
[28] B. Wang, L. Dai, Z. Wang, N. Ge, and S. Zhou, "Spectrum and energy-efficient beamspace MIMO-NOMA for millimeter-wave communications using lens antenna array," *IEEE J. Sel. Areas Commun.*, vol. 35, no. 10, pp. 2370–2382, Oct. 2017.
[29] W. Hao, M. Zeng, Z. Chu, and S. Yang, "Energy-efficient power allocation in millimeter wave massive MIMO with non-orthogonal multiple access," *IEEE Wireless Commun. Lett.*, vol. 6, no. 6, pp. 782–785, Dec. 2017.
[30] M. Zeng, A. Yadav, O. A. Dobre, G. I. Tsiropoulos, and H. V. Poor, "Capacity comparison between MIMO-NOMA and MIMO-OMA with multiple users in a cluster," *IEEE J. Sel. Areas Commun.*, vol. 35, no. 10, pp. 2413–2424, Oct. 2017.
[31] S. Yu, W. U. Khan, X. Zhang, and J. Liu, "Optimal power allocation for NOMA-enabled D2D communication with imperfect SIC decoding," *Phys. Commun.*, 2021, Art. no. 101296.
[32] M. S. Ali, H. Tabassum, and E. Hossain, "Dynamic user clustering and power allocation for uplink and downlink non-orthogonal multiple access (NOMA) systems," *IEEE Access*, vol. 4, pp. 6325–6343, 2016.
[33] Y. Saito, Y. Kishiyama, A. Benjebbour, T. Nakamura, A. Li, and K. Higuchi, "Non-orthogonal multiple access (NOMA) for cellular future radio access," in *Proc. IEEE 77th Veh. Technol. Conf.*, 2013, pp. 1–5.
[34] M. Diamanti, G. Fragkos, E. E. Tsiropoulou, and S. Papavassiliou, "Unified user association and contract-theoretic resource orchestration in NOMA heterogeneous wireless networks," *IEEE Open J. Commun. Soc.*, vol. 1, pp. 1485–1502, 2020.
[35] F. Fang, H. Zhang, J. Cheng, and V. C. Leung, "Energy-efficient resource allocation for downlink non-orthogonal multiple access network," *IEEE Trans. Commun.*, vol. 64, no. 9, pp. 3722–3732, Sep. 2016.
[36] H. Farhadi, C. Wang, and M. Skoglund, "Fixed-rate transmission over fading interference channels using point-to-point Gaussian codes," *IEEE Trans. Commun.*, vol. 63, no. 10, pp. 3633–3644, Oct. 2015.
[37] B. Liu, C. Liu, and M. Peng, "Resource allocation for energy-efficient MEC in NOMA-enabled massive IoT networks," *IEEE J. Sel. Areas Commun.*, vol. 39, no. 4, pp. 1015–1027, Apr. 2021.
[38] J. Zuo, Y. Liu, Z. Qin, and N. Al-Dhahir, "Resource allocation in intelligent reflecting surface assisted NOMA systems," *IEEE Trans. Commun.*, vol. 68, no. 11, pp. 7170–7183, Nov. 2020.
[39] L. P. Qian, Y. Wu, H. Zhou, and X. Shen, "Dynamic cell association for non-orthogonal multiple-access V2S networks," *IEEE J. Sel. Areas Commun.*, vol. 35, no. 10, pp. 2342–2356, Oct. 2017.
[40] N. Cheng et al., "Space/aerial-assisted computing offloading for IoT applications: A learning-based approach," *IEEE J. Sel. Areas Commun.*, vol. 37, no. 5, pp. 1117–1129, May 2019.
[41] J. Cui, Y. Liu, Z. Ding, P. Fan, and A. Nallanathan, "QoE-based resource allocation for multi-cell NOMA networks," *IEEE Trans. Wireless Commun.*, vol. 17, no. 9, pp. 6160–6176, Sep. 2018.
[42] L. Ruan et al., "Energy-efficient multi-UAV coverage deployment in UAV networks: A game-theoretic framework," *China Commun.*, vol. 15, no. 10, pp. 194–209, Oct. 2018.
[43] K. Wang, J. Cui, Z. Ding, and P. Fan, "Stackelberg game for user clustering and power allocation in millimeter wave-NOMA systems," *IEEE Trans. Wireless Commun.*, vol. 18, no. 5, pp. 2842–2857, May 2019.
[44] D. Sikeridis, E. E. Tsiropoulou, M. Devetsikiotis, and S. Papavassiliou, "Wireless powered public safety IoT: A UAV-assisted adaptive-learning approach towards energy efficiency," *J. Netw. Comput. Appl.*, vol. 123, pp. 69–79, 2018.
[45] R. Li et al., "Joint trajectory and resource allocation design for UAV communication systems," in *Proc. IEEE Globecom Workshops*, 2018, pp. 1–6.
[46] M. Gapeyenko, V. Petrov, D. Moltchanov, S. Andreev, N. Himayat, and Y. Koucheryavy, "Flexible and reliable UAV-assisted backhaul operation in 5G mmwave cellular networks," *IEEE J. Sel. Areas Commun.*, vol. 36, no. 11, pp. 2486–2496, Nov. 2018.
[47] Y. Zeng, R. Zhang, and T. J. Lim, "Throughput maximization for UAV-enabled mobile relaying systems," *IEEE Trans. Commun.*, vol. 64, no. 12, pp. 4983–4996, Dec. 2016.
[48] T. Başar and G. J. Olsder, *Dynamic Noncooperative Game Theory*. Philadelphia, PA, USA: SIAM, 1998.
[49] F. Zhou, Y. Wu, R. Q. Hu, and Y. Qian, "Computation rate maximization in UAV-enabled wireless-powered mobile-edge computing systems," *IEEE J. Sel. Areas Commun.*, vol. 36, no. 9, pp. 1927–1941, Sep. 2018.
[50] J. Wang, Z. Na, and X. Liu, "Collaborative design of multi-UAV trajectory and resource scheduling for 6g-enabled Internet of Things," *IEEE Internet Things J.*, vol. 8, no. 20, pp. 15096–15106, Oct. 2021.
[51] M. Grant, S. Boyd, and Y. Ye, "CVX: MATLAB software for disciplined convex programming, version 2.1 beta," 2014.
[52] N. Mokari, F. Alavi, S. Parsaeefard, and T. Le-Ngoc, "Limited-feedback resource allocation in heterogeneous cellular networks," *IEEE Trans. Veh. Technol.*, vol. 65, no. 4, pp. 2509–2521, Apr. 2016.
[53] H. Zhang et al., "Energy efficient dynamic resource optimization in NOMA system," *IEEE Trans. Wireless Commun.*, vol. 17, no. 9, pp. 5671–5683, Sep. 2018.

Maryam Hosseini received the B.Sc. degree in electronic engineering from the University of Isfahan, Isfahan, Iran, and the M.Sc. degree in communication engineering from Imam Reza University, Mashhad, Iran. She is currently working toward the Ph.D. degree in communication engineering from the University of Birjand, Birjand, Iran, under the supervision of Dr. Reza Ghazizadeh. In 2019, she joined KTH Royal Institute of Technology, Stockholm, Sweden, as a Visiting Researcher under the supervision of Dr. Hamed Farhadi and working on the neural networks. Her research interests include machine learning, neural communication systems, and wireless communications with focus on radio resource allocation, multiple access technology, and vehicular communication.

Reza Ghazizadeh received the B.S. and M.S. degrees in electrical engineering from the Ferdowsi University of Mashhad, Mashhad, Iran, in 1992 and 1996, respectively, and the Ph.D. degree in telecommunication engineering from Southwest JiaoTong University, Chengdu, China, in 2009. He is currently an Associate Professor with the Department of Electrical and Computer Engineering, University of Birjand, Birjand, Iran. His research interests include radio resource management, analysis and optimization in the next generation wireless networks, machine learning, and neural communication systems.